Table 1 Direction of optimal deflection impulse applied at interception

Interval between interception and close approach, days	$\hat{e}_R$	$\hat{e}_T$	$\hat{e}_N$
19	0.983	0.184	$<10^{-3}$
30	0.970	0.243	$<10^{-3}$
44	0.954	0.300	$<10^{-3}$
52	0.945	0.327	$<10^{-3}$
65	0.934	0.357	$<10^{-3}$
72	0.923	0.385	$<10^{-3}$
76	0.900	0.435	$<10^{-3}$
86	0.959	0.281	$<10^{-3}$
104	0.920	0.391	$<10^{-3}$
134	0.932	0.362	$<10^{-3}$

1998). The direction may be inferred from the magnitude of the components of a unit vector in the direction of the deflecting impulse $\delta\bar{v}_0$. The unit vectors are those of an asteroid-fixed radial, tangential, normal (to asteroid orbit plane) basis, shown in Fig. 1. For this example, the optimal deflecting impulse is mostly radial, but may have a significant tangential component. The deflection normal to the asteroid plane is always negligibly small. There is not a monotonic variation of the direction as time progresses, and this is probably because the direction is expressed on a moving basis.

Conclusions

Many of the strategies for amelioration of the danger of an asteroid's collision with the Earth involve, at the time of interception, applying a small impulsive velocity change to the asteroid. In this work we show how, using the asteroid orbit state transition matrix, this impulse should be applied to maximize the deflection of the asteroid at the time of close approach. The algorithm requires no explicit (numerical) optimization and is, thus, easily applied.We also find, for the case in which the asteroid will make less than one complete orbit of the sun before its close approach or impact with the Earth, that the deflection resulting from a given magnitude of impulse increases the earlier the asteroid is intercepted. It is, thus, legitimate for this case to optimize the interception trajectory, minimizing the flight time, and then optimize the direction of the deflecting impulse separately, to maximize the deflection of the asteroid at what would otherwise be the impact time.

One important result, illustrated in Fig. 2 for a very representative ECA, is that, if the interceptor spacecraft is launched less than a year in advance of the asteroid's possible collision with Earth, the deflection obtained will be on the order of an Earth diameter for every 1 m/s velocity change applied to the asteroid. When it is considered how many millions of kilograms of mass some of the ECA possess, it would be very difficult to change their velocity by even 1 m/s. Thus, it may only be feasible to deflect asteroids of moderate size if they can be reached several years in advance of a potential collision.

References

[1]"List of the Potentially Hazardous Asteroids (PHAs)," URL: http://cfa-www.harvard.edu/iau/lists/Dangerous.html [cited 31 July 2001].

[2]Ahrens, T. J., and Harris, A. W., "Deflection and Fragmentation of Near-Earth Asteroids," *Hazards Due to Comets and Asteroids*, edited by T. Gehrels, Univ. of Arizona Press, Tucson, AZ, 1994, pp. 897–928.

[3]Solem, J. C., and Snell, C. M., "Terminal Intercept for Less Than One Period Warning," *Hazards Due to Comets and Asteroids*, edited by T. Gehrels, Univ. of Arizona Press, Tucson, AZ, 1994, pp. 1013–1034.

[4]Conway, B. A., "Optimal Low-Thrust Interception of Earth-Crossing Asteroids," *Journal of Guidance, Control, and Dynamics,* Vol. 20, No. 5, 1997, pp. 995–1002.

[5]Park, S. Y., and Ross, I. M., Two-Body Optimization for Deflecting Earth-Crossing Asteroids, *Journal of Guidance, Control, and Dynamics,* Vol. 22, No. 3, 1999, pp. 415–420.

[6]Battin, R. H., *An Introduction to the Mathematics and Methods of Astrodynamics,* AIAA Education Series, AIAA, Washington, DC, 1994, pp. 463–467.

Rate Feedback Control of Free-Free Uniform Flexible Rod

Natalya Raskin* and Yoram Halevi†
Technion—Israel Institute of Technology, 32000 Haifa, Israel

I. Introduction

STATIC rate feedback is one of the simplest yet effective ways of controlling flexible structures. Its main purpose is to add damping, thus dissipating energy from the system, which is a key issue in vibration control. In servo systems the static rate feedback is sometimes used as an inner loop, providing a better-shaped "plant" for the outer loop, which enforces tracking.

It is well known[1] that a collocated structure with rate feedback is positive, that is, energy dissipating. Hence the system is stable, or asymptotically stable, if no rigid-body modes exist, regardless of the feedback gain value. However, one would like to find out what is the best, in some sense, gain. In certain cases collocated control may not be feasible. In others noncollocated control can be used intentionally because the area where vibration suppression is required and the actuation location do not coincide. Hence the properties of a system with noncollocated control are also of interest.

Infinite dimensional systems can be analyzed either in the frequency domain by using Nyquist stability criterion and similar tools[2] or by studying the poles pattern. References 3 and 4 contain an analysis of the pole location of flexible mechanical systems under noncollocated control. In this Note a similar approach is used for systems governed by the wave equation with static rate feedback. The relatively simple structure of such systems allows global results regarding the stability and the general shape of the poles map.

II. Transfer Function Derivation and Analysis

Consider the free-free uniform rod of length L subjected to torque moment $M(t)$ at one end, as shown in Fig. 1. $\theta(x,t)$ is a torsion angle at distance x from the forced end. The system is governed by the following wave equation and boundary conditions:

$$\frac{\partial^2\theta(x,t)}{\partial x^2} = \frac{1}{c^2}\frac{\partial^2\theta(x,t)}{\partial t^2} \tag{1}$$

$$GI_p\frac{\partial\theta(x,t)}{\partial x}\bigg|_{x=0} = -M(t), \qquad \frac{\partial\theta(x,t)}{\partial x}\bigg|_{x=L} = 0 \tag{2}$$

where I_p denotes the polar moment of inertia, G is the shear elasticity modulus, ρ is the material density, and $c=(G/\rho)^{1/2}$ is the wave propagation velocity. Laplace transform with respect to time converts the partial differential Eq. (1) into an ordinary one in x:

$$\frac{\partial^2\theta(x,s)}{\partial x^2} - \frac{s^2}{c^2}\theta(x,s) = 0 \tag{3}$$

The solution of Eq. (3) is

$$\theta(x,s) = C_1(s)\exp(sx/c) + C_2(s)\exp[-(sx)/c] \tag{4}$$

$C_1(s)$ and $C_2(s)$ can be calculated from the boundary conditions. Introducing the normalized coordinate $\beta = x/L$ and the time constant $\tau = L/c$, the following transfer function is obtained:

Received 26 May 2000; revision received 31 October 2000; accepted for publication 1 June 2001.

*Graduate Research Assistant, Faculty of Mechanical Engineering.

†Associate Professor, Faculty of Mechanical Engineering; merhy01@tx.technion.ac.il.

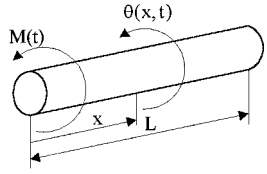

Fig. 1 Free-free uniform rod in torsion.

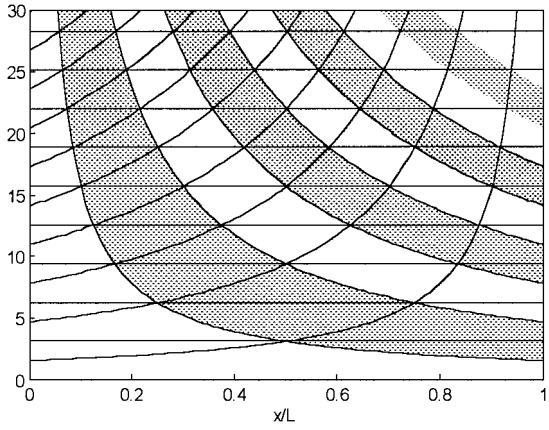

Fig. 2 Poles (——) and zeros (- - -) of $G(x,s)$ vs normalized sensor location.

$$\frac{\theta(x,s)}{M(s)} = \frac{c}{GI_p}\cdot\frac{1}{s}\cdot\frac{\exp[\tau(1-\beta)s]+\exp[-\tau(1-\beta)s]}{\exp(\tau s)-\exp(-\tau s)}$$

$$= \frac{c}{GI_p}\cdot\frac{1}{s}\cdot\frac{\exp[-2\tau(1-\beta)s]+1}{1-\exp(-2\tau s)}\cdot\exp(-\tau\beta s) \tag{5}$$

The expression $\tau\beta(=x/c)$ in the last term represents the time required for the wave to reach a point at a distance x. This is also the dead time in the response, which plays an important role in order reduction and control of flexible structures with noncollocated sensors and actuators.[5] The output of interest in this Note is the angular velocity $\omega(x,t)=\partial\theta(x,t)/\partial t$. In this case the integrator in the transfer function (5) is cancelled, and $G(x,s)$, the transfer function from the moment $M(t)$ to the angular velocity $\omega(x,t)$, is given by

$$G(x,s) = \frac{c}{GI_p}\cdot\frac{\exp[\tau(1-\beta)s]+\exp[-\tau(1-\beta)s]}{\exp(\tau s)-\exp(-\tau s)} \tag{6}$$

All the poles p_k and the zeros z_k of $G(x,s)$ are on the imaginary axis and are given as

$$p_k = \frac{k\pi}{\tau}j, \qquad z_k(\beta) = \frac{\left(k+\frac{1}{2}\right)\pi}{\tau(1-\beta)}j \qquad k=0,\pm1,\pm2,\ldots \tag{7}$$

The poles do not depend on the sensor location β because they are global property of the system. The zeros positions, on the other hand, are inversely proportional to $(1-\beta)$. When the sensor and the actuator are collocated, i.e., $\beta=0$, the zeros alternate with the poles, and each zero lies exactly in the middle between two neighboring poles. As the distance between the sensor and the actuator increases, the distance between zeros increases as well. This fact is the source to the well-known phenomenon that in a noncollocated transfer function an antiresonance may or may not exist between two resonance frequencies. Finally, for $\beta=1$ the system has no finite zeros. Figure 2 shows the poles and the zeros of the open-loop system, normalized by $1/\tau$, as a function of β . An intersection of the zeros and poles curves indicates a cancellation of that pole. This occurs at nodes of the corresponding eigenfunctions. The meaning of the shaded areas will be explained in the next section.

III. General Rate Feedback

The main goal of this Note is to study the behavior of the closed-loop system, which is obtained when the static rate feedback control law

$$M(t) = -K\omega(\beta,t) \tag{8}$$

is applied to the system (1). Of particular interest is the poles pattern as a function of the rate feedback gain K and the sensor location β.

Stability

The closed-loop characteristic equation is

$$I + KG(x,s) = 0 \tag{9}$$

A key point in the root locus type analysis, which will be invoked, is the following lemma, which is an extension of a known result for finite dimensional systems. Because of space limitations, it is given without a proof.

Lemma 1: Let $G(s)=g(s)/f(s)$, where $f(s)$ and $g(s)$ are analytical functions of the complex variable s. If $\lim_{s\to\infty} sG(s)=0$, then the sum of all of the roots of

$$f(s)+\alpha g(s)=0 \tag{10}$$

is a constant independent of α.

The sum of all of the open-loop poles ($K=0$) is zero. It is easily shown that for any $\beta\neq0$, $G(x,s)$ satisfies the condition of lemma 1. Hence it follows from the lemma that if a certain pole moves to the left-half plane there must be at least one pole that moves to the right-half plane, causing instability. It can be shown that there are no poles on the imaginary axis at any finite frequency. Hence a pole that moves into the right-half plane (RHP) will stay there. The conclusion from lemma 1 is therefore as follows: Any noncollocated static rate feedback destabilizes the system (1) and (2).

In practice the structure has always a low level of damping. The definite theoretical conclusion then means that stability is maintained only for a narrow range of low gains. Such a case has been considered by Yang,[3] and our conclusions agree with the results there, which were developed for a general controller.

Closed-Loop Poles Pattern

For further investigation of the closed-loop poles location, we write the characteristic equation (9) explicitly as

$$\exp(\tau s)-\exp(-\tau s)+A\{\exp[\tau(1-\beta)s]+\exp[-\tau(1-\beta)s]\}=0 \tag{11}$$

where $A=Kc/GI_p$ is the normalized rate feedback gain. Differentiating with respect to A and evaluating at a pole s_k leads to

$$\frac{ds_k}{dA} = -\frac{\exp[\tau(1-\beta)s_k]+\exp[-\tau(1-\beta)s_k]}{\tau[\exp(\tau s_k)+\exp(-\tau s_k)]+A(1-\beta)\tau\{\exp[\tau(1-\beta)s_k]-\exp[-\tau(1-\beta)s_k]\}} \tag{12}$$

At $A=0$, where $s_k=p_k$, Eq. (15) becomes

$$\left.\frac{ds_k}{dA}\right|_{A=0} = -\frac{1}{\tau}\cos(\beta\pi k) \tag{13}$$

This result is in agreement with lemma 1, showing that for any $\beta\neq0$ there exist open-loop poles for which the derivative is positive, thus moving into the RHP. The derivative is real, meaning that all loci depart perpendicularly to the imaginary axis. It is easily shown that as A approaches infinity the derivative (12) goes to zero. To see the direction along which the root locus approaches the open-loop zeros, we divide the characteristic equation (11) by A and define $\hat{A}=A^{-1}$. Differentiating with respect to $\hat{A}$ and evaluating at $\hat{A}=0$, $s_k=z_k$, we obtain

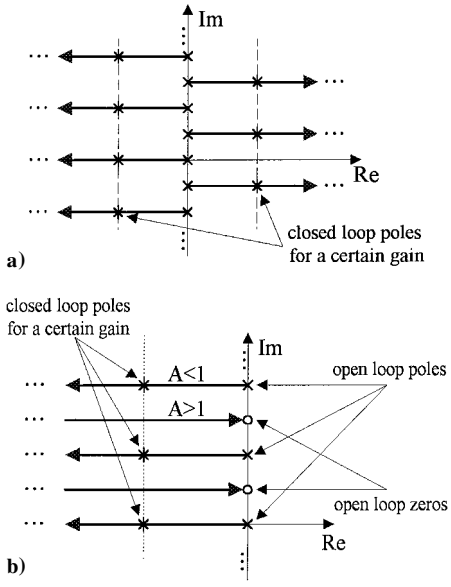

Fig. 3 Root locus for a) $\beta = 1$ and b) $\beta = 0$.

$$\left.\frac{ds_k}{d\hat{A}}\right|_{\hat{A}=0} = -\frac{1}{(1-\beta)\tau}\cos\left[\frac{\beta}{1-\beta}\pi\left(k+\tfrac{1}{2}\right)\right] \tag{14}$$

Because for $\beta = 1$ the system has no zeros, this expression is always finite. First notice that, as in Eq. (13), this quantity is real, hence the root locus arrives at the zeros perpendicular to the imaginary axis. Recalling that $\hat{A}$ is reciprocal to A, we have

$$\operatorname{sign}\left\{\lim_{A\to\infty}\frac{ds_k}{dA}\right\} = \operatorname{sign}\left\{\cos\left[\frac{\beta}{1-\beta}\pi\left(k+\tfrac{1}{2}\right)\right]\right\} \tag{15}$$

where a negative sign indicates that the root locus approaches the zero from the right. From Eqs. (13) and (15) it is possible to see if a pole (zero) is the beginning (end) of a branch that goes into the RHP. The shaded areas in Fig. 3 contain all of the poles and zeros belonging to such branches.

Special Case: Sensor at $\beta = 1$

For $\beta = 1$ the characteristic equation (14) is as follows:

$$\exp(-2\tau s) - 2A\exp(-\tau s) - 1 = 0 \tag{16}$$

This is a quadratic equation in $\exp(-\tau s)$ with the following solutions:

$$\exp(-\tau s) = A \pm \sqrt{A^2+1} \tag{17}$$

The closed-loop poles, which are the solutions of Eqs. (20), are then

$$s_k = (-1)^{k+1}(1/\tau)\,\ell n\left\{A+\sqrt{A^2+1}\right\} \pm (\pi k/\tau)j \qquad k = 0, 1, 2\ldots \tag{18}$$

The branches of root locus, beginning at the even open-loop poles (including $k = 0$), go to the left with constant imaginary part and the same real part. The branches, originating from the odd open-loop poles, go to the right with constant imaginary part too and with the same rate as the even branches. Because the system does not have any zeros, these horizontal straight lines go to infinity. Figure 3a summarizes the results for this case.

IV. Collocated Rate Feedback

For $\beta = 0$ the characteristic equation is given by

$$1 - \exp(-2\tau s) + A[1+\exp(-2\tau s)] = 0 \tag{19}$$

Hence $\exp(-2\tau s) = (1+A)/(1-A)$, and the poles are given as

$$s_k = \begin{cases} -\dfrac{1}{2\tau}\,\ell n\left\{\dfrac{1+A}{1-A}\right\} \pm \dfrac{\pi k}{\tau}j & k = 0, 1, 2, \ldots \text{ for } A < 1 \\ -\dfrac{1}{2\tau}\,\ell n\left\{\dfrac{A+1}{A-1}\right\} \pm \dfrac{\pi\left(k-\frac{1}{2}\right)}{\tau}j & k = 1, 2, \ldots \text{ for } A > 1 \end{cases} \tag{20}$$

Notice that for $A < 1$ the system has one real pole, but for $A > 1$ it disappears.

Equation (20) has several interesting properties:

1) All of the closed-loop poles are in the open left-half plane for all $0 < A < \infty$.

2) The real parts of all of the closed-loop poles are the same.

3) Except for the jump at $A = 1$, the imaginary parts, which are the damped natural frequencies, are constant and independent of the gain A. For $A < 1$ they are identical with the natural frequencies of the open-loop free-free system and for $A > 1$ with those of a clamped-free rod.

4) For $A < 1$ the absolute value of the (negative) real parts increases with A, and for $A > 1$ it decreases when A increases. Furthermore, the real parts for A and for A^{-1} are the same.

The physical interpretation of these results is as follows:

1) It is in accordance with the well-known result[1] that collocated rate feedback stabilizes the system for all $A > 0$.

2) It means that all modes have the same settling time, i.e., they decay at the same rate. This phenomenon, called uniform damping, was shown to be attractive in terms of the control effort vs performance tradeoff.[6,7]

3) It can be thought off in the same way because no effort is spent on changing the natural frequencies.

4) It implies that the damping ratio increases (settling time decreases) with the rate feedback gain up to a certain point, and then decreases until for an infinite gain the system does not have damping at all and behaves like an open-loop clamped-free rod. The same phenomenon has been observed and studied in Ref. 8 for beams in bending.

For $A = 1$ all poles go to infinity. Clearly this is the optimal feedback gain for which, at least theoretically, the settling time consists only of the unavoidable delays. Returning to dimensional parameters, $A = 1$ corresponds to

$$K = GI_p/c = I_p G^{\frac{1}{2}}\rho^{\frac{1}{2}} \tag{21}$$

This value depends only on the material properties and the cross section and is independent of the length L and consequently of the overall inertia of the rod.

In the root locus of a finite dimensional approximation of the system or in case the system has some damping, the poles do not go to infinity for the optimal gain, but it still corresponds, or very close, to the edge point of all branches. As the order of the approximation increases, the root locus is getting closer to the one in Fig. 3b.

V. Conclusions

The stability properties and the closed-loop poles location of free-free flexible rods under rate feedback control were investigated. It was shown that systems with noncollocated rate feedback are always unstable. For collocated static-rate feedback it was shown that there exists an optimal gain, which eliminates the system dynamics. The optimal gain depends only on the material and cross-section properties of the flexible system and is independent of its length and consequently of its inertia. The damped natural frequency is piecewise constant and changes only at the optimal gain.

References

[1] Balas, M. J., "Direct Velocity Feedback Control of Large Space Structures," *Journal of Guidance and Control*, Vol. 2, No. 3, 1979, pp. 252, 253.

[2] Chait, Y., Radcliffe, C. J., and MacCluer, C. R., "Frequency Domain Stability Criterion for Vibration Control of a Bernoulli-Euler Beam," *Journal of Dynamic Systems, Measurement and Control*, Vol. 110, No. 3, 1988, pp. 303–307.

[3] Yang, B., "Noncolocated Control of a Damped String Using Time Delay,"

Journal of Dynamic Systems, Measurement and Control, Vol. 114, No. 4, 1992, pp. 736–740.

[4]Yang, B., and Mote, C. D., Jr., "On Time Delay in Noncolocated Control of Flexible Mechanical Systems," *Journal of Dynamic Systems, Measurement and Control*, Vol. 114, No. 3, 1992, pp. 409–415.

[5]Raskin, N., and Halevi, Y., "Control of Flexible Structures Using Models with Dead Time," *Proceedings of the 7th Institute of Electrical and Electronics Engineers Mediterranean Conference on Control and Automation*, IEEE Publications, Piscataway, NJ, 1999, pp. 782–794.

[6]Silverberg, L., "Uniform Damping Control of Spacecraft," *Journal of Guidance, Control, and Dynamics*, Vol. 9, No. 2, 1986, pp. 221–227.

[7]Rossetti, D. J., and Sun, J. Q., "Uniform Modal Damping of Rings by an Extended Node Control Theorem," *Journal of Guidance, Control, and Dynamics*, Vol. 18, No. 2, 1995, pp. 373–375.

[8]Balakrishnan, A. V., "Theoretical Limits of Damping Attainable by Smart Beams with Rate Feedback," *Proceedings of SPIE's Annual Symposium on Smart Structures and Materials: Mathematics and Control in Smart Structures*, edited by V. V. Varadan and J. Chandra, Vol. 3039, International Society for Optical Engineering, Bellingham, WA, 1997, pp. 205–214.

Reducing Minimum Time for Flexible Body Small-Angle Slewing with Vibration Suppression

Arun K. Banerjee*
Lockheed Martin Advanced Technology Center, Palo Alto, California 94304

Introduction

INPUT commands for slewing a flexible body in minimum time are often preshaped to suppress residual vibration after slewing. The procedure is to convolve the bang-bang command for minimum time slew for a rigid body with a three impulse sequence[1] designed to suppress the vibration of the actual, flexible body. The resulting slew extends the rigid-body minimum time by the period of vibration. A method of input shaping that does not extend the rigid-body minimum time has recently been proposed,[2] and it does so by increasing the torque level so as to reduce the rigid-body minimum time by the period of vibration. In the case of rapid slewing of a relatively soft flexible body through a small angle, it may happen that the vibration period is longer than the rigid-body minimum time, and then this method becomes inapplicable. This Note shows two exact methods to reduce the minimum time for rest-to-rest small-angle slewing in such situations. The first method is new and consists of scaling the torque following convolution, and the second method is similar to those in Refs. 3–5, except that it does not require using an optimization code. The methods are robust and illustrated with systems having one or two vibration modes to suppress. Application of the methods may be as diverse as in disk drive positioning and spacecraft precision slewing.

Scaling of Convolved Torque

Consider first a system, with one vibration mode to suppress, represented by two rigid rotors of inertia J_1, J_2 connected by a massless elastic shaft of stiffness K. Let $J_1 = 1.0$, $J_2 = 0.1$ kg-m^2, and $K = 4.3426$ N-m/rad, so that the time period of vibration is 10 s. Minimum time bang-bang control for a rigid body is described by the torque time function,

$$\begin{aligned} \tau_b &= T_{\max}, && 0 \le t \le t_{\min}/2 \\ &= -T_{\max}, && t_{\min}/2 < t \le t_{\min} \\ &= 0, && t > t_{\min} \end{aligned} \tag{1}$$

where the minimum time for slewing to an angle θ_f is given by

$$t_{\min} = 2\sqrt{J_t \theta_f / T_{\max}} \tag{2}$$

For $\theta_f = 1$ deg and the total rigid-body inertia in this case $J_t = 1.1$, the minimum time is 8 s for a maximum torque $T_{\max} = 0.0012$ N-m. This is a case where the rigid-body slewing time is less than the vibration period. Input shaping to suppress the vibration that would be generated by the bang-bang torque consists in doing a convolution of the time function of Eq. (1) with the three impulse sequence time function given in Table 1, where the function values are zero except at the indicated time points.

This convolution is symbolically represented as follows:

$$T = \tau_b^* F_1 \tag{3}$$

The top plot in Fig. 1 shows the result of the convolved torque in this numerical case. The key point to note is that the maximum torque used is less than the available maximum torque. In fact, it can be shown that the torque used is less than the available maximum whenever the period of vibration to be suppressed is greater than half the minimum time for a rigid body. This suggests the idea that a new solution can be sought by scaling up the original maximum torque, thereby reducing the rigid-body minimum time so that after convolution with the three impulse sequence the actual required maximum torque equals the available maximum torque. The factor by which the maximum torque has to be scaled up depends on the result of the convolution. The torque factor (available torque/maximum torque after convolution) is two in this case, and the result of the scaled and convolved torque is shown as the middle plot in Fig. 1. The corresponding time plots of the slew angle in the two cases of unscaled and scaled torques are shown in the bottom plot of Fig. 1. It is seen that scaling the torque has reduced the minimum time.

Although simple linear scaling works if only one mode shaping is involved, this does not work for multimode vibration suppression. To see this, consider a three-degree-of-freedom system of three rigid bodies connected by two mass-less elastic beams. The bodies are of moments of inertia J_1, J_2, and J_3, and the beams are of bending stiffnesses K_1 and K_2. The system is undergoing planar slewing

Table 1 Function F_i representing three impulse sequence for vibration of period T_i

t	F_i
0	0.25
$T_i/2$	0.5
T_i	0.25

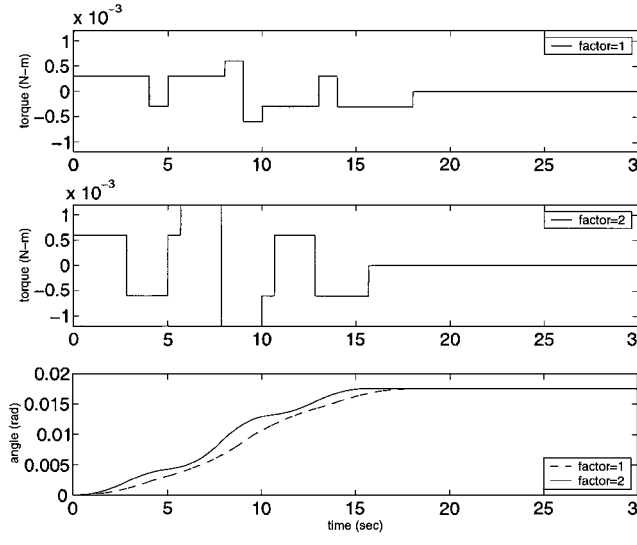

Fig. 1 Scale factored convolution torques and the slewing-angle response for one-mode shaping.

Received 2 January 2001; revision received 16 April 2001; accepted for publication 22 April 2001.

*Consulting Scientist, L9-24/201.